THE JOURNAL OF PHYSICAL CHEMISTRY B

Article

pubs.acs.org/JPCB

Ion Transport with Charge-Protected and Non-Charge-Protected Cations Using the Compensated Arrhenius Formalism. Part 2. Relationship Between Ionic Conductivity and Diffusion

Matt Petrowsky,[†] Allison Fleshman,[†] Dharshani N. Bopege,[‡] and Roger Frech*[,†]

[†]Department of Chemistry and Biochemistry, University of Oklahoma, 101 Stephenson Parkway, Norman, Oklahoma 73019, United States

[‡]Homer L. Dodge Department of Physics and Astronomy, University of Oklahoma, 440 W. Brooks St., Norman, Oklahoma 73019, United States

ABSTRACT: Temperature-dependent ionic conductivities and cation/anion self-diffusion coefficients are measured for four electrolyte families: TbaTf-linear primary alcohols, LiTf-linear primary alcohols, TbaTf-*n*-alkyl acetates, and LiTf-*n*-alkyl acetates. The Nernst−Einstein equation does not adequately describe the data. Instead, the compensated Arrhenius formalism is applied to both conductivity and diffusion data. General trends based on temperature and alkyl chain length are observed when conductivity is plotted against cation or anion diffusion coefficient, but there is no clear pattern to the data. However, plotting conductivity exponential prefactors against those for diffusion results in four distinct curves, one each for the alcohol and acetate families described above. Furthermore, the TbaTf-alcohol and TbaTf-acetate data are "in line" with each other. The conductivity prefactors for the LiTf-alcohol data are smaller than those for the TbaTf data. The LiTf-acetate data have the lowest conductivity prefactors. This trend in prefactors mirrors the observed trend in degree of ionic association for these electrolytes.

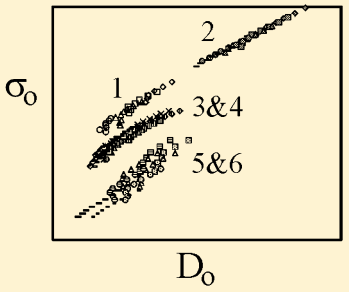

INTRODUCTION

Hydrodynamic theory is often used to describe mass and charge transport in liquid electrolytes.[1−7] In hydrodynamic theory the movement of a particle in solution is hindered by the resistive drag exerted by the solvent, and consequently the solution viscosity is used to quantify this resistive force. Hydrodynamic theory is often utilized to relate the ionic conductivity of an electrolyte to the diffusion coefficients of the cation and anion, but the predicted results are often substantially different from those obtained experimentally. In fact, the discrepancy between the theoretical and experimental ionic conductivity is often used as a measure of the ionic association in the electrolyte.[7−10] Recently, the compensated Arrhenius formalism (CAF) has been postulated as an alternative to hydrodynamic theory to describe mass and charge transport in pure liquids and liquid electrolytes.[11−16] The CAF assumes transport to be a thermally activated process that is mediated by relaxation of the solvent. Instead of viscosity, the solution static dielectric constant, ε_s, is the parameter that characterizes transport. The temperature-dependent ionic conductivity and diffusion coefficient assume an Arrhenius-like expression that also includes a dielectric constant dependence in the exponential prefactor.

Part I of this series used the CAF to explain the temperature-dependent ionic conductivity data of moderately concentrated tetrabutylammonium trifluoromethanesulfonate (TbaTf) and lithium trifluoromethanesulfonate (LiTf) alcohol electrolytes.[16] The CAF has been successful in describing the temperature dependence of self-diffusion coefficients for pure polar solvents.[15] Here, the CAF is applied to cation and anion diffusion coefficients for the same solutions studied in part I as well as for some moderately concentrated acetate electrolytes. The CAF results are then used to relate the ionic conductivity to the ion diffusion coefficients.

EXPERIMENTAL SECTION

All chemicals (≥99% pure) were obtained from either Aldrich or Alfa Aesar and used as received. The chemicals were stored and all samples were prepared in a glovebox (≤1 ppm H_2O) under a nitrogen atmosphere. The liquid electrolytes were made at ambient glovebox temperature (approximately 27 °C) by dissolving salt into solvent until the appropriate molal concentration (mol salt/kg solvent) was obtained, followed by stirring for 24 h.

The capacitance (C) and conductance (G) were measured using an HP 4192A impedance analyzer that swept a frequency range from 1 kHz to 13 MHz. The sample holder was an Agilent 16452A liquid test fixture. The conductivity σ is calculated from the measured conductance G through the equation $\sigma = LGA^{-1}$, where L is the electrode gap and A is the electrode area. The static dielectric constant ε_s is calculated from the measured capacitance C through the equation $\varepsilon_s = \alpha C C_o^{-1}$, where α is a variable to account for stray capacitance

Received: February 1, 2012
Revised: June 7, 2012
Published: July 30, 2012

   dx.doi.org/10.1021/jp3010585 | *J. Phys. Chem. B* 2012, 116, 9303−9309

and C_o is the atmospheric capacitance.[17] A Huber ministat 125 bath was used to regulate the temperature from 5 to 85 °C, in increments of 10 °C. Additional details of the conductivity/dielectric constant instrumentation and method of data analysis have been previously given.[11]

For diffusion measurements the samples were contained in 5 mm OD and 20 cm long glass NMR tubes sealed with parafilm. The sample height in the NMR tube was constricted to 0.8 cm. Self-diffusion coefficients were measured using a Varian VNMRS-400 MHz NMR spectrometer equipped with an Auto-X-Dual Broadband 5 mm probe. The corresponding Larmor frequencies for ^{1}H, ^{19}F, and ^{7}Li are 399.87, 376.22, and 155.40 MHz, respectively. An FTS XR401 Air-Jet regulator was used to control the temperature in the measurement range from 5 to 85 °C. The gradient field strength was calibrated from literature diffusion coefficient values for ethanol.[18] The diffusion measurements were made using the Stejskal-Tanner pulsed field gradient NMR spin−echo technique.[19] For a given gradient duration and interval, the attenuation of the signal intensity was recorded as a function of the gradient field strength over the range 6−62 G/cm. Plotting the logarithm of intensity versus the square of the gradient field strength produced a linear relationship whose slope was used to determine the diffusion coefficient.[20]

RESULTS AND DISCUSSION

CAF Analysis of Ion Diffusion Coefficients. Diffusion coefficients of ions and solvent molecules are commonly measured using pulsed field gradient NMR. Figure 1 shows

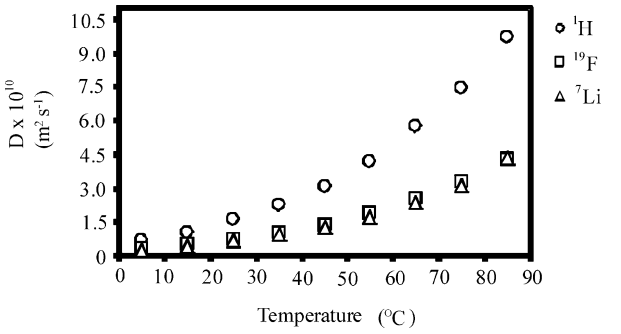

Figure 1. Diffusion coefficient (^{1}H, ^{19}F, and ^{7}Li) versus temperature for 0.30 *m* LiTf-1-hexanol.

temperature-dependent diffusion coefficients for the solvent (^{1}H), cation (^{7}Li), and anion (^{19}F) for 0.30 *m* LiTf-1-hexanol. The diffusion coefficients of the cation and anion are very close in value across the temperature range, whereas those for the solvent increase more rapidly with increasing temperature than either the cation or anion diffusion coefficients. These same trends are often observed in other liquid electrolytes.[8,9,21,22]

The CAF analysis has been successfully applied to self-diffusion coefficients of pure liquids, and it is equally applicable to solvent diffusion in 0.30 *m* TbaTf or LiTf 1-alcohol solutions. However, the focus here is determining if CAF behavior is observed for cation and anion diffusion. The diffusion coefficient D may be written in a form explicitly emphasizing the postulates of the CAF:[12,15]

$$D = D(T, \varepsilon_s) = D_o(\varepsilon_s(T)) \exp(-E_a/RT) \quad (1)$$

where E_a is the energy of activation, ε_s is the static dielectric constant, and $D_o(\varepsilon_s(T))$ is the exponential prefactor for diffusion. The compensated Arrhenius equation (CAE) is

$$\ln\left(\frac{D(T, \varepsilon_s)}{D_r(T_r, \varepsilon_s)}\right) = -\frac{E_a}{RT} + \frac{E_a}{RT_r} \quad (2)$$

where $D_r(T_r, \varepsilon_s)$ is the reference diffusion coefficient measured at the reference temperature T_r. CAF behavior is observed if a graph of $\ln(D(T, \varepsilon_s)/D_r(T_r, \varepsilon_s))$ versus $1/T$ is linear. Figure 2

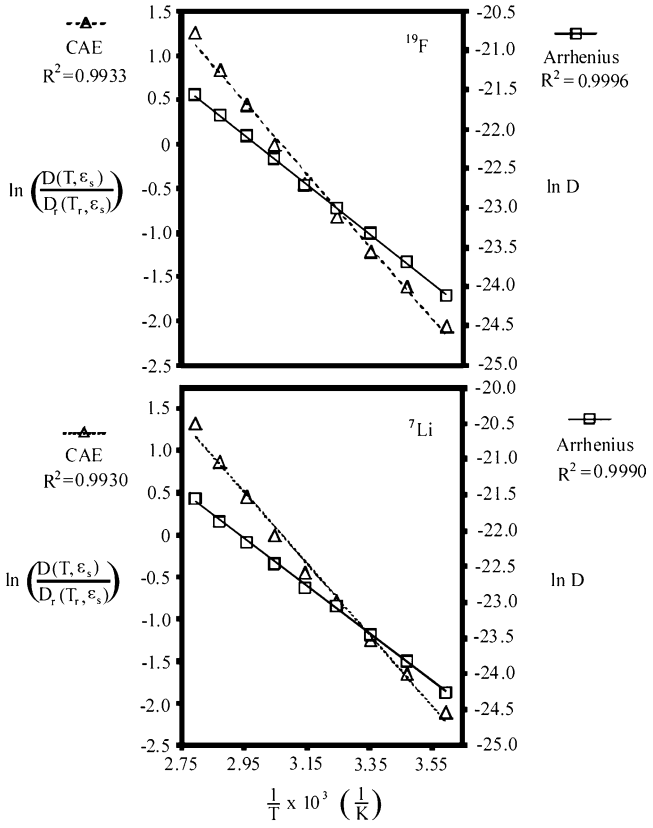

Figure 2. Simple Arrhenius and compensated Arrhenius plots for lithium and fluorine diffusion coefficients for 0.30 *m* LiTf-1-hexanol.

depicts both simple Arrhenius and compensated Arrhenius plots for lithium and fluorine diffusion coefficients for 0.30 *m* LiTf-1-hexanol. The CAE reference temperature was 55 °C, and the reference diffusion coefficient curve consisted of 0.30 *m* LiTf solutions of 1-butanol, 1-pentanol, 1-hexanol, 1-heptanol, and 1-octanol. Contrary to the LiTf conductivity data described in part I, the simple Arrhenius plots for both the lithium and fluorine diffusion coefficients are linear. The simple Arrhenius E_a values for lithium and fluorine are 27.5 ± 0.3 and 26.2 ± 0.2 kJ/mol, respectively. Even though simple Arrhenius behavior is observed for these data, the CAF must still be applied. Our previous work has shown that using an E_a value obtained from a simple Arrhenius plot does not result in a master curve when the exponential prefactors are plotted against ε_s.[11,15,23] The CAF activation energies for lithium from the slope and intercept are 35.0 ± 1 and 35.3 ± 1 kJ/mol, respectively, whereas those for fluorine are 34.1 ± 1 and 34.3 ± 1 kJ/mol, respectively.

The diffusion coefficient for the Tba cation could not be measured due to overlapping solvent peaks and therefore only

dx.doi.org/10.1021/jp3010585 | J. Phys. Chem. B 2012, 116, 9303−9309

anion and solvent diffusion coefficient data were collected for TbaTf electrolytes. However, it is informative to know if the large charge-protected Tba cation diffuses in a similar manner as the triflate anion. This information can be readily obtained by dissolving TbaTf in a completely deuterated solvent so that there are no interfering peaks. Table 1 shows that the cation

Table 1. Cation and Anion Diffusion Coefficients Measured at Four Different Temperatures for 0.30 *m* TbaTf-Ethanol-d_6

temp (°C)	diffusion coefficient (m^2 s^{-1}) ^{1}H (Tba cation)	diffusion coefficient (m^2 s^{-1}) ^{19}F (triflate anion)	percent difference between cation and anion diffusion coefficients
5	2.06×10^{-10}	2.17×10^{-10}	5.2
15	2.71×10^{-10}	2.84×10^{-10}	4.7
25	3.54×10^{-10}	3.68×10^{-10}	3.9
35	4.45×10^{-10}	4.70×10^{-10}	5.5

and anion diffusion coefficients have similar values at each temperature in 0.30 *m* TbaTf-ethanol-d_6. It is well-known that TbaTf exists solely as "free" ions in solution on the time scale of IR spectroscopy;[16,24−27] therefore, the magnitudes of the Tba and triflate diffusion coefficients are expected to be close in value in order to maintain electroneutrality in solution.

Average CAF activation energies for 0.30 *m* LiTf and TbaTf 1-alcohol electrolytes are given in Table 2 for the conductivity

Table 2. Average CAF Activation Energies from Both Conductivity and Diffusion Coefficient Data for 0.30 *m* LiTf and TbaTf 1-alcohol solutions

salt	average E_a (kJ/mol)
Conductivity Data	
LiTf	25.8 ± 0.9
TbaTf	43.3 ± 0.8
Diffusion Coefficient Data	
LiTf (^{7}Li)	35.1 ± 1
LiTf (^{19}F)	35.1 ± 1
LiTf (^{1}H)	35.4 ± 0.9
TbaTf (^{19}F)	40.6 ± 1
TbaTf (^{1}H)	39.4 ± 0.7

data presented in part I as well as for diffusion data for the cation (^{7}Li), anion (^{19}F), and solvent (^{1}H). All five alcohol members contribute to the average E_a values in Table 2. The reference temperature is chosen such that the temperature-dependent dielectric constant data for each member lie within the dielectric constant range of the reference curve. The diffusion activation energies for cation, anion, and solvent are very similar to each other for the LiTf solutions. However, the conductivity E_a value for LiTf alcohols is markedly lower than those for diffusion. The TbaTf alcohol solutions have a conductivity E_a value that is comparable to the diffusion E_a values observed for the anion and solvent.

The exponential prefactor for diffusion is determined from eq 1 by dividing the temperature-dependent diffusion coefficients by the Boltzmann factor $\exp(-E_a/RT)$. The top half of Figure 3 shows that when the lithium diffusion coefficients are plotted against dielectric constant for 0.30 *m* LiTf-1-alcohol solutions the data are grouped into five curves similarly to the conductivity data described in Figure 9 of part I. However, the bottom half of Figure 3 shows that when the lithium diffusion exponential prefactors are graphed versus the dielectric constant all data lie on a master curve. It should be

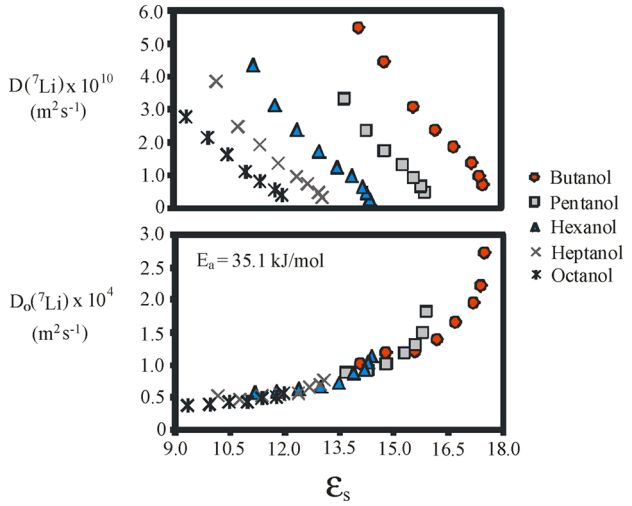

Figure 3. Diffusion data for 0.30 *m* LiTf-1-alcohol (alcohol = butanol, pentanol, hexanol, heptanol, or octanol). Top half: lithium diffusion coefficients versus dielectric constant. Bottom half: lithium diffusion exponential prefactors versus dielectric constant.

noted that the low temperature pentanol data deviate slightly from the master curve. The fluorine diffusion data are similar to the lithium diffusion data in the 0.30 *m* LiTf-alcohol electrolytes (see Figure 1).

The top half of Figure 4 plots fluorine diffusion coefficients against dielectric constant for 0.30 *m* TbaTf-1-alcohols.

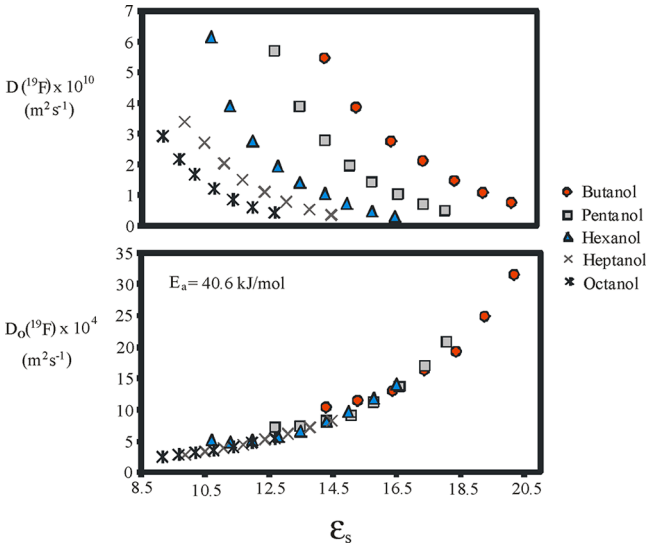

Figure 4. Diffusion data for 0.30 *m* TbaTf-1-alcohol (alcohol = butanol, pentanol, hexanol, heptanol, or octanol). Top half: fluorine diffusion coefficients versus dielectric constant. Bottom half: fluorine diffusion exponential prefactors versus dielectric constant.

Although the data consist of five separate curves, the qualitative dielectric constant dependence of the diffusion coefficients differs somewhat from the corresponding plot for the LiTf-alcohol solutions. The bottom half of Figure 4 shows that a master curve results when the exponential prefactors are plotted against the dielectric constant for the 0.30 *m* TbaTf-1-alcohol solutions.

dx.doi.org/10.1021/jp3010585 | J. Phys. Chem. B 2012, 116, 9303−9309

Nernst–Einstein Equation. Hydrodynamic theory relates conductivity and diffusion through the Nernst–Einstein equation[1,9,28]

$$\sigma = \frac{nq^2}{kT}(D_+ + D_-) \quad (3)$$

where σ is the conductivity, n is the number density of ions, q is the ion charge, k is Boltzmann's constant, T is temperature, and D_+ and D_- are the cation and anion diffusion coefficients, respectively. A graph of σT versus $(D_+ + D_-)$ should be linear if eq 3 describes the data, assuming the number density of ions does not change substantially with temperature. Figure 5 shows

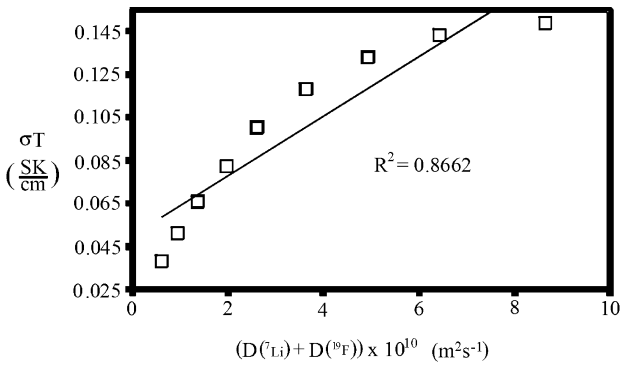

Figure 5. Graph of σT versus $(D(^7Li) + D(^{19}F))$ for 0.30 m LiTf-1-hexanol over the temperature range 5–85 °C.

that this kind of graph produces substantially nonlinear behavior for 0.30 m LiTf-1-hexanol over the temperature range 5–85 °C. The conductivity calculated from eq 3 is often much greater than the experimentally measured conductivity, and this is usually attributed to ionic association effects.[28] It was demonstrated in part I that both free ions and ion pairs exist in 0.30 m LiTf-1-alcohol solutions and therefore the curvature in Figure 5 might be expected. Figure 6 shows that TbaTf

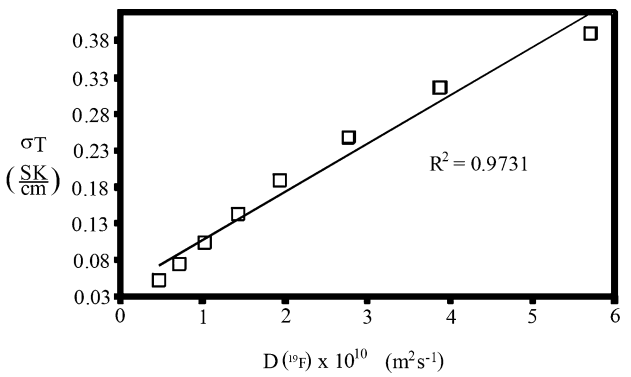

Figure 6. Graph of σT versus $D(^{19}F)$ for 0.30 m TbaTf-1-pentanol over the temperature range 5–75 °C.

electrolytes have the same general qualitative behavior that is observed in Figure 5. However, TbaTf cannot form contact ion pairs or aggregates due to the charge-protected nature of the Tba cation,[24–27] and therefore, attribution of the observed behavior to ionic association effects is either wrong or at the very least incomplete. Deviations from the Nernst–Einstein equation have been reported in a variety of systems other than organic liquid electrolytes. For example, Boden et al. attributed the observed deviations in solutions of LiTf in poly(ethylene oxide) to correlated motions of cations and anions.[29] To achieve self-consistency in their study of gel electrolytes based on cross-linked poly(ethylene oxide), Aihara et al. modified the Nernst–Einstein equation using a multiplicative factor to account for the degree of ion association.[30] The effect of organic diluents such as vinylene carbonate, ethylene carbonate, tetrahydrofuran and toluene on ion transport in ionic liquid electrolytes was carried out using the Nernst–Einstein equation.[31] It has been argued that deviations observed in the Nernst–Einstein equation for molten salts and ionic liquids are due to differences in cross-correlation functions of ionic velocities rather than ionic association.[32] Instead of ionic association, it is quite possible that deviations in the Nernst–Einstein equation result from the assumptions underlying Einstein's relationship between diffusion coefficient D and mobility μ: $D = \mu kT/q$. This relationship forms the basis for the Nernst–Einstein equation and it is only valid to the extent by which Einstein's equation accurately describes the relationship between diffusion and mobility. Bockris has noted that the diffusion coefficient and molar conductivity have different dependencies, so if the Nernst–Einstein equation is valid at one concentration then it cannot be valid at any other concentration.[1] Furthermore, it is informative to consider transport in systems where ionic association plays no role. For example, it is well-known that electronic transport in crystalline semiconductors can often be accurately described with Einstein's equation. However, disordered semiconductors show substantial deviations from this equation.[33–39]

Relationship Between Ionic Conductivity and Diffusion Coefficients Using the CAF. As an alternative to the Nernst–Einstein equation, the CAF is used to examine the relationship between conductivity and diffusion. Figure 7 shows

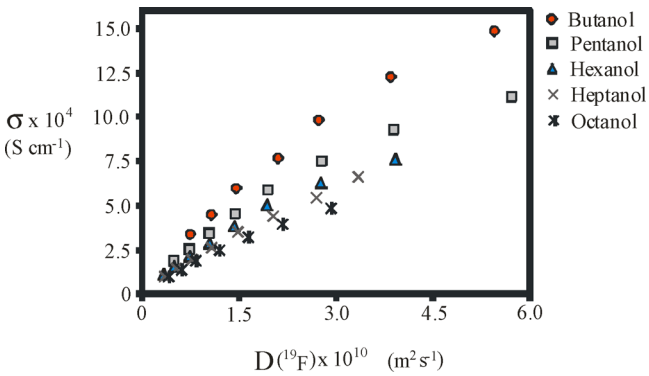

Figure 7. Conductivity versus anion diffusion coefficient for 0.30 m TbaTf-1-alcohol (alcohol = butanol, pentanol, hexanol, heptanol, or octanol).

conductivity versus anion diffusion coefficient for 0.30 m TbaTf-1-alcohol electrolytes. The data are separated into five curves, with each curve representing the temperature-dependent data for a given alcohol member. The topmost curve is for the electrolyte with the shortest alkyl chain (butanol). Increasing the alkyl chain length decreases the placement of the curve.

An interesting correlation is observed if the exponential prefactor for conductivity is plotted against that for diffusion. Figure 8 shows such a graph for the 0.30 m TbaTf-1-alcohol data. All data appear to fall on the same curve when the

dx.doi.org/10.1021/jp3010585 | J. Phys. Chem. B 2012, 116, 9303–9309

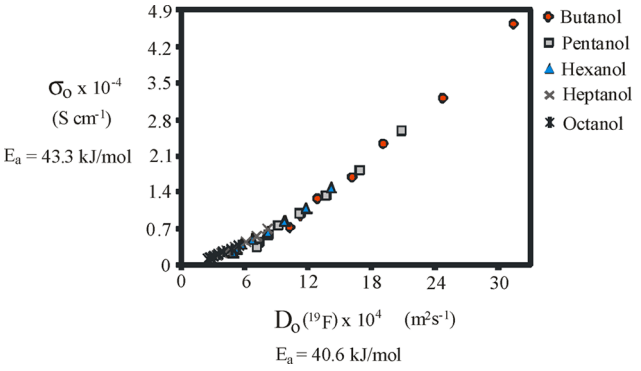

Figure 8. Conductivity exponential prefactor versus anion diffusion exponential prefactor for 0.30 *m* TbaTf-1-alcohol (alcohol = butanol, pentanol, hexanol, heptanol, or octanol). The average activation energy for conductivity is 43.3 kJ/mol, whereas that for anion diffusion is 40.6 kJ/mol.

prefactors for conductivity are plotted against those for anion diffusion.

Figure 9 plots conductivity versus diffusion coefficient for 0.30 *m* solutions of TbaTf-*n*-acetates, LiTf-*n*-acetates, TbaTf-1-alcohols, and LiTf-1-alcohols. Both the *x* and *y* axes are on a logarithmic scale. A few general trends can be observed. For each solution, both conductivity and diffusion coefficient increase with temperature as expected. Within each solvent family (e.g., linear alcohols) both conductivity and diffusion coefficients decrease as the chain length increases. The conductivities for the LiTf-acetate solutions are much lower than those for the other electrolytes. Aside from these general trends, there is no clear pattern to the data. However, Figure 10 shows that plotting the conductivity prefactors versus diffusion prefactors results in four distinct curves. Two curves consist of the TbaTf-alcohol and TbaTf-acetate data, and two curves result from the LiTf-alcohol and LiTf-acetate data. It should be noted that the TbaTf-acetate data (group 1) appear to be "in line" with the TbaTf-alcohol data (group 2). A possible explanation for the behavior observed in Figure 10 is given in the Summary and Conclusions section.

SUMMARY AND CONCLUSIONS

The CAF was originally applied to ionic conductivity data, and here it is shown that it also describes the temperature dependence of ion diffusion coefficients in organic liquid electrolytes. The question that naturally arises then is what is the relationship between ionic conductivity and cation and anion diffusion coefficients in an electrolyte? Figures 8 and 10 show that the data for a particular electrolyte family (e.g., TbaTf-alcohols, LiTf-alcohols, TbaTf-acetates, and LiTf-acetates) all fall on a single curve when the prefactors for conductivity are plotted against those for diffusion, although more scatter is observed in the LiTf-acetate data (Figure 10). This phenomenon probably originates from the fact that the conductivity prefactors and diffusion prefactors are both functions of a common variable: the solution static dielectric constant. More importantly, the roughly parallel behavior of the six sets of data in Figure 10 strongly suggests that both the conductivity prefactor and the diffusion coefficient prefactor have the same functional dependence on ε_s.

The relative placement of the four curves in Figure 10 is also intriguing. This placement follows the observed trend in ionic association for these electrolytes. TbaTf electrolytes consist only of free ions due to the charge-protected nature of the Tba cation. Both sets of TbaTf data in Figure 10 (groups 1 and 2) appear to fall on the same line, and this line has higher conductivity prefactors (for a given value of the diffusion prefactor) than any of the LiTf data. The LiTf-alcohol data in Figure 10 (groups 3 and 4) fall below the TbaTf data. It was demonstrated in part I that 0.30 *m* LiTf-1-alcohol solutions contain ion pairs, but that the majority of salt exists as free ions. The LiTf-acetate data in Figure 10 (groups 5 and 6) have the lowest conductivity prefactors. Current studies are underway to examine the extent of ionic association in LiTf-acetate electrolytes, although preliminary results indicate a high degree of association. A very small fraction of the salt exists as free ions, while the majority of species are ion pairs and higher

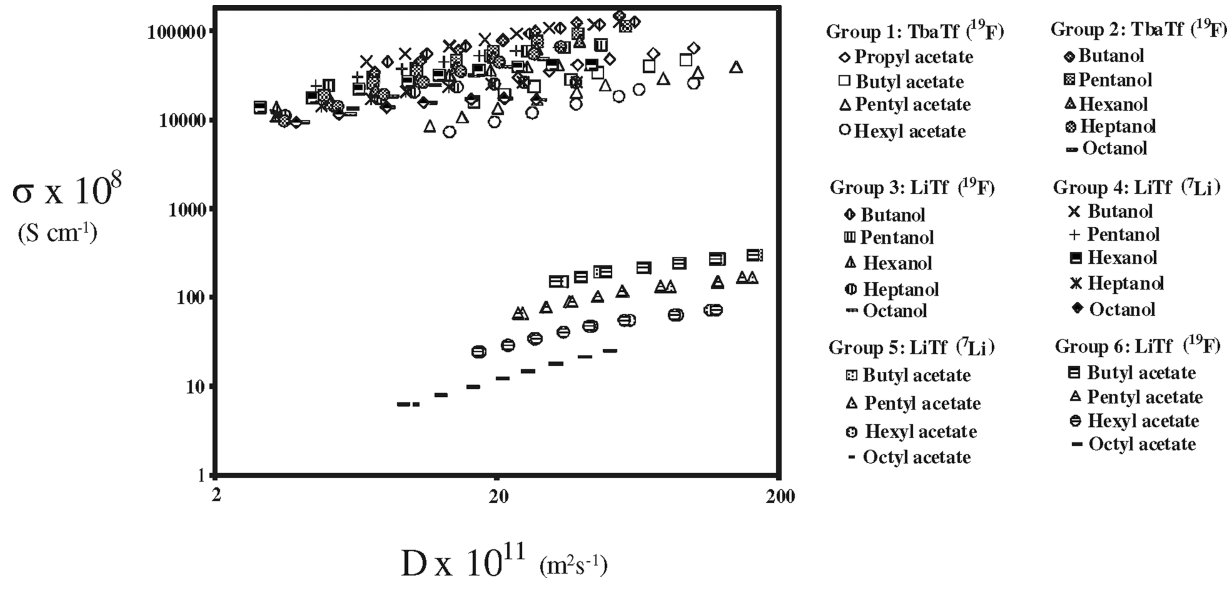

Figure 9. Conductivity versus cation and anion diffusion coefficients for 0.30 *m* solutions of TbaTf-*n*-acetates, LiTf-*n*-acetates, TbaTf-1-alcohols, and LiTf-1-alcohols over the temperature range 5−85 °C. Both axes are depicted on a logarithmic scale.

dx.doi.org/10.1021/jp3010585 | J. Phys. Chem. B 2012, 116, 9303−9309

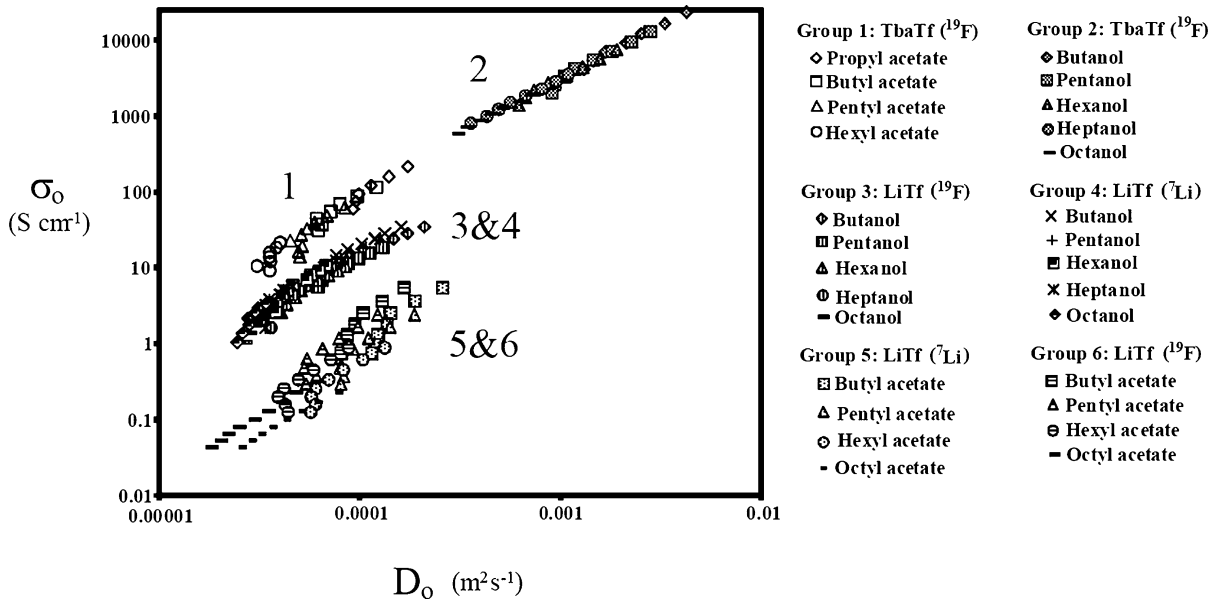

Figure 10. Conductivity exponential prefactor versus diffusion coefficient exponential prefactors for 0.30 *m* solutions of TbaTf-*n*-acetates, LiTf-*n*-acetates, TbaTf-1-alcohols, and LiTf-1-alcohols over the temperature range 5−85 °C. Both axes are depicted on a logarithmic scale.

aggregates. Therefore, it is possible that the placement of the data in a conductivity prefactor versus diffusion prefactor plot gives valuable information about the degree of ionic association in the electrolyte. However, more data from other solvent families must be collected in order to determine the validity of this claim. In particular, it is important to see whether additional TbaTf-solvent data fall on the line observed in Figure 10 for TbaTf-alcohols and TbaTf-acetates.

AUTHOR INFORMATION

Notes

The authors declare no competing financial interest.

ACKNOWLEDGMENTS

We wish to thank Army Research Office for support of this work through Grant No. W911NF-10-1-0437. We are grateful to Dr. Susan Nimmo for her guidance with the NMR diffusion measurements and acknowledge the National Science Foundation for its financial support of the NMR equipment (Grant No. CHE#0639199). We thank the Johnson research group in the OU physics department, and especially Jeremy Jernigen, for their help with glovebox modifications. We appreciate the expertise of Chris Crowe in software development for the HP 4192A. Finally, we thank Whitney Booher for her help with diffusion coefficient data collection.

REFERENCES

(1) Bockris, J.; Reddy, A. *Modern Electrochemistry*, 2nd ed.; Plenum Press: New York, 1998; sections 4.4.7−4.4.12, Vol. *1*.
(2) Levine, I. *Physical Chemistry*, 5th ed.; McGraw-Hill: New York, 2002; Chapter 16.
(3) Nelson, R. D., Jr.; Smyth, C. P. *J. Phys. Chem.* **1964**, *68*, 2704−2708.
(4) Zhu, X. X.; Macdonald, P. M. *Macromolecules* **1992**, *25*, 4345−4351.
(5) Edward, J. T. *J. Chem. Educ.* **1970**, *47*, 261−270.
(6) Iwahashi, M.; Ohbu, Y.; Kato, T.; Suzuki, Y.; Yamauchi, K.; Yamaguchi, Y.; Muramatsu, M. *Bull. Chem. Soc. Jpn.* **1986**, *59*, 3771−3774.
(7) Hayamizu, K.; Aihara, Y.; Arai, S.; Martinez, C. G. *J. Phys. Chem. B* **1999**, *103*, 519−524.
(8) Ward, I. M.; Boden, N.; Cruickshank, J.; Leng, S. A. *Electrochim. Acta* **1995**, *40*, 2071−2076.
(9) Williamson, M. J.; Southall, J. P.; Hubbard, H. V. A., St.; Johnston, S. F.; Davies, G. R.; Ward, I. M. *Electrochim. Acta* **1998**, *43*, 1415−1420.
(10) Aihara, Y.; Bando, T.; Nakagawa, H.; Yoshida, H.; Hayamizu, K.; Akiba, E.; Price, W. *J. Electrochem. Soc.* **2004**, *151*, A119−A122.
(11) Fleshman, A.; Petrowsky, M.; Jernigen, J.; Bokalawela, R. S. P.; Johnson, M.; Frech, R. *Electrochim. Acta* **2011**, *57*, 147−152.
(12) Petrowsky, M.; Frech, R. *J. Phys. Chem. B* **2009**, *113*, 5996−6000.
(13) Petrowsky, M.; Frech, R. *J. Phys. Chem. B* **2009**, *113*, 16118−16123.
(14) Petrowsky, M.; Frech, R. *Electrochim. Acta* **2010**, *55*, 1285−1288.
(15) Petrowsky, M.; Frech, R. *J. Phys. Chem. B* **2010**, *114*, 8600−8605.
(16) Petrowsky, M.; Fleshman, A.; Frech, R. *J. Phys. Chem. B* **2012**, *116*, 5760−5765.
(17) *Agilent 16452A Liquid Test Fixture Operation and Service Manual*; Agilent Technologies: Santa Clara, CA, 2000.
(18) Rathbun, R. E.; Babb, A. L. J. *Phys. Chem.* **1961**, *65*, 1072−1074.
(19) Stejskal, E. O.; Tanner, J. E. *J. Chem. Phys.* **1965**, *42*, 288−292.
(20) Price, W. S. *Concepts Magn. Reson.* **1997**, *9*, 299−336.
(21) Hayamizu, K.; Matsuo, A.; Arai, J. *J. Electrochem. Soc.* **2009**, *156*, A744−A750.
(22) Ferry, A.; Oradd, G.; Jacobsson, P. *Electrochim. Acta* **1998**, *43*, 1471−1476.
(23) Bopege, D.; Petrowsky, M.; Fleshman, A.; Frech, R.; Johnson, M. *J. Phys. Chem. B* **2012**, *116*, 71−76.
(24) Frech, R.; Huang, W. *J. Solution Chem.* **1994**, *23*, 469−481.
(25) Frech, R.; Huang, W.; Dissanayake, M. *Mater. Res. Soc. Symp. Proc.* **1995**, *369*, 523−534.
(26) Bacelon, P.; Corset, J.; Loze, C. *J. Solution Chem.* **1983**, *12*, 13−22.
(27) Bacelon, P.; Corset, J.; Loze, C. *J. Solution Chem.* **1983**, *12*, 23−31.
(28) Ward, I. M.; Williamson, M. J.; Hubbard, H. V. A., St.; Southall, J. P.; Davies, G. R. *J. Power Sources* **1999**, *81*−*82*, 700−704.
(29) Boden, N.; Leng, S. A.; Ward, I. M. *Solid State Ionics* **1991**, *45*, 261−270.

(30) Aihara, Y.; Arai, S.; Hayamizu, K. *Electrochim. Acta* **2000**, *45*, 1321−1326.
(31) Bayley, P.; Lane, G.; Rocher, N.; Clare, B.; Best, A.; MacFarlane, D.; Forsyth, M. *Phys. Chem. Chem. Phys.* **2009**, *11*, 7202−7208.
(32) Harris, K. *J. Phys. Chem. B* **2010**, *114*, 9572−9577.
(33) Nguyen, T.; O'Leary, S. *Appl. Phys. Lett.* **2003**, *83*, 1998−2000.
(34) Mansurova, S.; Stepanov, S.; Camacho-Pernas, V.; Ramos-Garcia, R.; Gallego-Gomez, F.; Mecher, E.; Meerholz, K. *Phys. Rev. B* **2004**, *69*, 193203−1−193203−4.
(35) Tripathi, A.; Tripathi, D.; Mohapatra, Y. *Phys. Rev. B* **2011**, *84*, 041201−1−041201−4.
(36) Tal, O.; Epstein, I.; Snir, O.; Roichman, Y.; Ganot, Y.; Chan, C. K.; Kahn, A.; Tessler, N.; Rosenwaks, Y. *Phys. Rev. B* **2008**, *77*, 201201−1−201201−4.
(37) Barkai, E.; Fleurov, V. N. *Phys. Rev. E* **1998**, *58*, 1296−1310.
(38) Richert, R.; Pautmeier, L.; Bassler, H. *Phys. Rev. Lett.* **1989**, *63*, 547−550.
(39) Berlin, Y. A.; Siebbeles, L. D. A.; Zharikov, A. A. *Chem. Phys. Lett.* **1999**, *305*, 123−131.